JETIR.ORG ISSN: 2349-5162 | ESTD Year : 2014 | Monthly Issue
JOURNAL OF EMERGING TECHNOLOGIES AND INNOVATIVE RESEARCH (JETIR)
An International Scholarly Open Access, Peer-reviewed, Refereed Journal

CHEMISTRY OF SULFATHIAZOLE AND 2,4-DIHYDROXYBENZALDEHYDE SCHIFF-BASE AND TOXICITY ASSESMENT AGAINST *C. Vulgaris* MICROCHLOROPHYTE

R. K. Abd Al Galil [1], E. M. Saad[1]. S. I. Mostafa [2*]

[1] *Chemistry Dept., Faculty of Science, Suez University, Egypt.*

[2] *Chemistry Dept., Faculty of Science, Mansoura University, Mansoura, Egypt.*

Corresponding Author: S. I. Mostafa

ABSTACT

H_2sdhb-Schiff base from sulfathiazole and 2,4- dihydroxybenzaldehyde, and its VO^{2+}, Co(II) and Ni(II) complexes were characterized by phsico-chemical measurements. H_2sdhb coordinates the metal ions through the N_{azom} and phenolic-O^- atoms, in mononegative bidentate manner. The toxicity of H_2sdhb and its complexes against the microchlorophyte (*C. vulgaris*) were tested and discussed with a comparison to the free metal ions, VO^{2+}, Co(II) and Ni(II).

Keywords: Schiff-base, H_2sdhb, Sulfathiazole, Complexes, Microchlorophyte, Metal ions

INTRODUCTION

Sulfa drugs are known as chemotherapeutic, can prevent microorganisms' infections [1]. They are known as antibiotics for thyroid, hypoglycaemic, diuretic, inhibitor agents against tumor cells, and many other activities [2-6]. Schiff-bases derived from sulfonamides are promising pharma compounds for toxicity based on the sulfonamide moiety. They are containing N, O, S, which have effective role in the field of drug discovery [7].

The octahedral complexes of Mn(II), Co(II), Ni(II), Cu(II), and Zn(II) with sulfathiazole and 5-nitrosalicylaldehyde Schiff base have been synthesized and their structures have been discussed. The Schiff-

base coordinate the metal ions in mononegative bidentate behaviour *via* azomethine-N and 2-hydroxy-O^- after deprotonation [8].

The biologically active tetrahedral Cu(II), Co(II), Ni(II), Mn(II) and Zn(II) complexes of Schiff-base (sulfathiazole- resorcinol) were prepared and their anticancer activity against human liver (HepG-2) and breast (MCF-7) carcinoma cells discussed [9]. The complexes of the divalent, Co, Ni, and Cu containing sulfathiazole-salicylaldehyde Sciff-base have been reported. The ligand chelates the metal ions via $N_{azomith}$, $N_{thiazole}$ and deprotonated phenolic-O^- atoms in tridentate character [10]. *o,p*-Dichlorosalicylaldehyde-sulfamethoxazole and *o,p*-dichlorosalicylaldehyde-sulfathiazole Schiff-bases Cu(II) complexes were prepared and X-ray crystal structural of the later one was measured and discussed [11]. The antimicrobial activity of Mn(II), Co(II), Ni(II) and Cu(II) complexes containing Schiff-bases prepared from sulfathiazole and doethylamino-2-hydroxybenzaldehyde have been tested and discussed [12]. Ramadan et al [13] prepared and investigated a series of Ni(II) Schiff-bases derived from sulfonamide Ni(II) complexes [13].

In this research article, sulfathiazole and 2,4-dihydroxybenzaldehyde Schiff-base (H_2sdhb; Fig. 1) and its Co(II), Ni(II) and VO^{2+} complexes were prepared and characterized by (IR, ^{1}H NMR, UV–vis, ESR and mass) spectroscopy, elemental analysis, conductivity, and TGA-analysis and magnetic measurements. Their Toxicity Assessment against *Chlorella Vulgaris* Microchlorophyte was also tested and discussed.

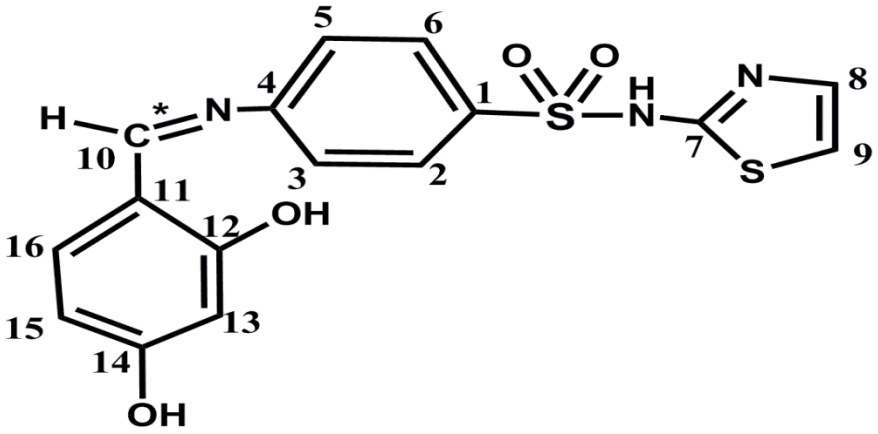

Fig. 1: **Schjiff-base from 2,4-dihydroxybenzaldehyde & Sulfathiazole (H_2sdhb)**

EXPERIMENTAL

MATERIAL & INSTRUMENTATION

Chemicals and solvents were obtained from sigma, Alfa Aesar and merk, and used as received. *C. vulgaris* was provided as a gift from Phycology Lab, Faculty of Science, Mansoura University, was grown on BG-11 nutrient medium [14].

FT-IR spectra were measured on a Matson5000 FT-IR spectrometer (4000–500 cm^{-1}), Elemental analyses, (C, H, N, S), carried out by The Microanalytical Unit and TGA made using Ni and NiCo as references, on a model Q500Analyzer TGA- 50 instrument; in the 20–1000° C range at a heating rate of 20° C min^{-1} (Cairo University, Egypt). UV-vis spectra in DMSO were measured using Hewlett-Packard 8453 spectrophotometer (Suez University, Egypt). NMR spectra were obtained by Varian Mercury 500-MHz spectrometer in DMSO-d6 solutions using TMS as the reference, while molar conductivity carried out in DMF at room temperature on a YSI Model 32 conductivity bridge. Magnetic moments (25° C) were recorded by a Johnson Matthey magnetic susceptibility balance with $Hg[Co(SCN)_4]$ as calibrant (Mansoura University, Egypt). Mass spectra (ESI-MS) were measured by LCQ Duo-MS25RFA instruments (McGill University, Canada). ESR spectrum was carried out on a Bruker EMX spectrometer working in the X-band (9.78 GHz) with 100 KHz modulation frequency. The microwave powder and modulation amplitudes were set at 1 mW and 4 Gauss, respectively. The low field signal was obtained after 4 scans with 10 fold increase in the receiver again. A powder spectrum was obtained in a 2mm quartz capillary at room temperature.

PREPARATION

- H_2sdhb

MeOH solution of 2,4-dihydroxybenzaldehyde (0.138 g, 1 mmol; 2 mL) was mixed with sulfathiazole (0.255 g, 1 mmol) in MeOH (10 mL) with adding 4 drops of Glacial AcOH. The obtained mixture was refluxed for 6 h. The yellow product was filtered off, washed with hot MeOH, Et_2O and dried over $CaCl_2$. Yield: 42%; mp 158° C.

- **[M(Hsdhb)$_2$(H$_2$O)$_2$] (M(II) = Co, Ni)**

Anhydrous Co(AcO)$_2$.4H$_2$O or Ni(AcO)$_2$.4H$_2$O (0.25 mmol) in EtOH (3 mL) was mixed with H$_2$sdhb (0.098 g, 0.25 mmol) in EtOH containing KOH (0.014 g, 0.25 mmol; 10 mL). The solution was heated with reflux for 6-8 hs. The obtained solutions were evaporated in air and brown (Co) or green (Ni) precipitate was obtained. It was filtered off, washed with EtOH and dried *in vacuo*. Yield: 78% (Co) and 73% (Ni). Conductivity (10^{-3} M in DMF): Λ_M = 18.0 (Co), 14.4 (Ni) ohm^{-1} cm^2 mol^{-1}

- **[VO(Hsdhb)$_2$]**

VO(SO4).H2O (0.042 g, 0.25mmol) in EtOH (10 mL) was mixed with H$_2$sdhb (0.098 g, 0.25 mmol) in EtOH (10 mL). The reaction mixture was refluxed for 8 hs to produce a green solid. It was filtered off, washed with water, EtOH, and dried in *vacuo*. Yield: 64%, Conductivity (10^{-3} M in DMF): Λ_M = 3.1 ohm^{-1} cm^2 mol^{-1}.

Toxicity Assessment against the Microchlorophyte (Chlorella Vulgaris)

The toxicity of the prepared complexes was tested, the standard instructions of the microalgae growth inhibition test according to OECD guideline for testing of chemicals No. 201 [15]. The growth inhibition test using *Chlorella vulgaris* (test alga was grown on BG-11 nutrient medium [16]) at light intensity equivalent to 4200 Lux using cool white uniform fluorescent illumination for 72 h incubation with 24 h sample interval. The growth was carried out and determined by using manual-cell counting by standard hemocytometer, which was illustrated as cell yield at the end of the incubation period, log cell number along the incubation period (24 hr. interval), and the relative cell count along incubation period to estimate the value of IC$_{50}$ for each treatment). The variables that affecting the growth of *Chlorella vulgaris* were illustrate by the average specific growth rate (***eq. 1***),

$$\mathbf{r = (ln\ N_l - lnN_0) / t_l - t_0} \qquad \mathbf{(1)}$$

where, r, T$_0$ and T$_L$ are the growth rate, start test time and the end of the time interval, respectively. Both N$_0$ and N$_L$ are the nominal initial cell density and the measured cell density at time t$_L$, respectively. The inhibition percentage (I) was obtained by applying ***eq. 2***,

$$\mathbf{I\% = (1 - N)/N_0) \times 100} \qquad \mathbf{(2)}$$

where, N_0 and N are the cell densities (cells per mL) in the control and treated cultures, respectively. The relative cell number (RCN; ***eq. 3***)

$$\mathbf{RCN = [N_{72}/ N_0] \times 100} \quad \mathbf{(3)}$$

where, N_{72} and N_0 are the cell densities in the treated cultures after 72h and the control, respectively. The 50% effective concentration (EC_{50}) of the treated samples, which is the concentration corresponding to the point where I, which is 50% on the inhibition curve and the toxic unit (***eq. 4***)

$$\mathbf{TU = [1/ EC_{50}] \times 100} \quad \mathbf{(4)}$$

RESULTS AND DISCUSSION

The elemental analysis (Table 1) and spectroscopic analysis are in agreement with the assigned formulae. Molar conductivities (Λ_M) in DMF at room temperature suggest all the complexes are non-electrolytes [16,17].

STRUCTURE CHARACTERIZATION

FTIR

The IR spectrum of sulfathiazole shows bands at 3350, 3320 cm^{-1} due to $\nu_{as}(NH_2)$ and $\nu_s(NH_2)$ stretches, respectively [18], these bands were not observed on the Schiff-base with the appearance of new band at 1640 cm^{-1}, due to Schiff-base formation [19-21]. The bands at 1620 and 1576 cm^{-1} attributed to the thiazole ν(C=N) stretches, which were shifted to lower energy and overlapped with ν(CH) stretches, based on weak H-bond formation [22]. The coordination of the azomethine N-atom to metal ion shifted the ν(HC=N) stretches to lower wave numbers [19-21]. This band in the complexes was shifted as well as the band at 1245 cm^{-1} (in the free ligand) assigned to the ν(C-O) stretch [19,20], which shifted to lower wave number, due to the coordination to the metal ions. In addition, in the complexes, the thiazole ν(C=N), $\nu_{as}(SO_2)$ and $\nu_s(SO_2)$ stretches, are not affected [13]. Fig. 2 shows the structures of $[M(Hsdhb)_2(H_2O)_2]$ (M(II) = Co, Ni) complexes.

Table 1: Elemental analysis data of H_2sdhb and its complexes

Compound	Elemental analysis (%) Found (Calcd.)				
	C	H	N	S	M
H_2sdhb	48.74 (48.85)	3.64 (3.82)	10.41 (10.69)	16.19 (16.28)	
[Co(Hsdhb)$_2$(H_2O)$_2$]	45.66 (45.56)	3.09 (3.32)	9.80 (9.97)	15.02 (15.19)	8199 (6.99)
[Ni(Hsdhb)$_2$(H_2O)$_2$]	45.59 (45.57)	3.12 (3.32)	9.78 (9.97)	15.09 (15.19)	6.69 (6.96)
[VO(Hsdhb)$_2$]	47.02 (47.12)	2.78 (2.95)	10.21 (10.31)	15.60 (15.71)	

The spectra of the complexes show new bands near 550 and 420 cm^{-1}, due to ν(M–O) and ν(M–N) stretches, respectively [19,20,23]. In case of [VO(Hsdhba)$_2$] (Fig. 3), a new band was observed at 973 cm^{-1}, characteristic to ν(VO), and confirm monomeric square-pyramidal VO^{2+} complexes [24].

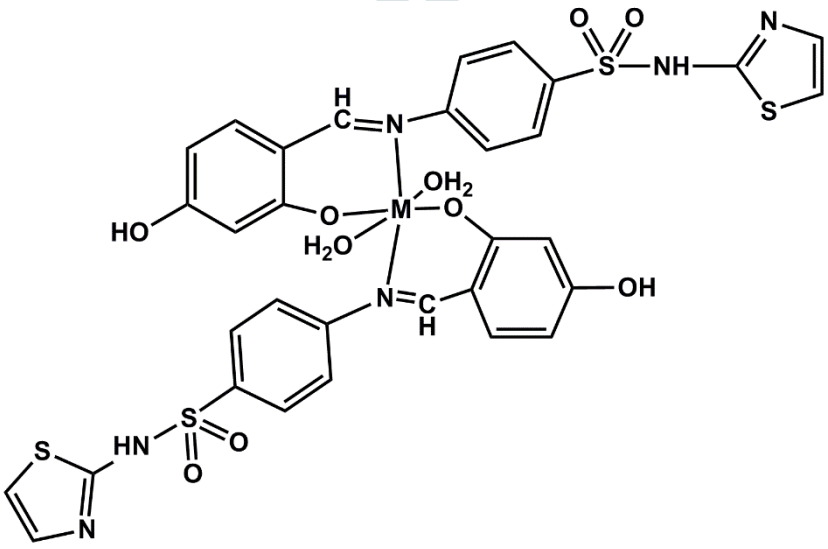

Fig. 2: Structure of [M(Hsdhb)$_2$(H_2O)$_2$] (M(II) = Co, Ni) complexes.

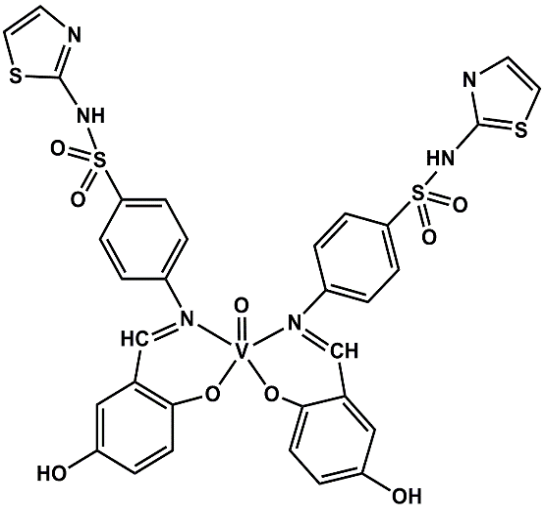

Fig. 3: Structure of [VO(Hsdhba)$_2$]

^{1}H-NMR

^{1}H-NMR spectrum of H_2sdhb and was recorded in DMSO-d_6. The azomethine (HC=N), NH, O(2)H and O(4)H protons show sharp singlets at δ 9.90, 12.58, 13.63 and 13.58 ppm, respectively. A group of doublets in δ 6.30-7.57 ppm assigned to the aromatic ring protons [18,25].

UV-Vis

The spectrum of the H_2sdhb in DMSO shows bands at 243 and 331 nm due to n → π* and π → π*, respectively [18,22]. The d-d spectra of [Co(Hsdhb)$_2$(H_2O)$_2$] (Fig. 4) and [Ni(Hsdhb)$_2$(H_2O)$_2$] can be assigned to transitions in octahedral ligand fields. The assignments of the Co(II): 622 ($^4T_{1g}$ → $^4A_{2g}$), 500 ($^4T_{lg}$ → $^4T_{lg}$ (P)), while For Ni(II): 635 ($^3A_{2g}$ → $^3T_{lg}$), 390 ($^3A_{2g}$ → $^3T_{lg}$(P)). The ligand field parameters are (10 D q = 8600 cm^{-1}, B = 907 cm $^{-1}$), and 4 (10 D q = 9800 cm -1, B = 800 cm -1), respectively. They are lying within the ranges reported for high-spin, octahedral Co(II) and N i(II) complexes with N ,O-chelating atoms [26]. The room temperature effective magnetic moments (μ_{eff}) for Co(II) and Ni(II) complexes are 2.81 and 2.10, respectively, which are less than the corresponding spin only, high spin values. This feature may be due to antiferromagnetic exchange interactions.

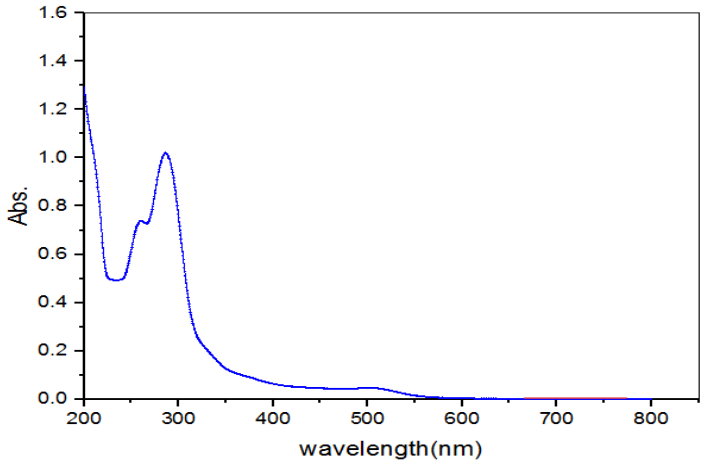

Fig. 4: UV-vis spectrum of $[Co(Hsdhb)_2(H_2O)_2]$

The electronic spectrum of the paramagnetic complex, $[VO(Hsdhba)_2]$, shows bands at 727, 601 and 493 nm due to $^2B_{2(d_{xy})} \rightarrow {}^2E(d_{xz},d_{yz})$, $^2B_2(d_{xy}) \rightarrow {}^2B1(d_{x2-y2})$ and charge transfer (LMCT) transitions in a square-pyramidal configuration [24], with magnetic moment of 1.66 B.M due to one electron [24].

ESR

ESR spectra are important tools for studying metal ion environment in the complexes (geometry, nature of the ligand active sites and degree of covalency of the metal ligand bonds). ESR spectrum of solid mononuclear VO^{+2} ion (S = 1/2, I = 7/2) has a characteristic octet, shows the hyperfine coupling to ^{51}V nuclear magnetic moment, while the presence of two vanadyl ions, two electron spins may combine to a non-magnetic spin singlet (S = 0) or a paramagnetic spin triplet state (S = 1) is observed.

Solid state ESR spectrum of $[VO(Hsdhb)_2]$ (RT; 300K), has C_{2v} point group (Figs. 3, 5) has a broad single line with eight-line pattern (poorly resolved), indicating mononuclear VO^{+2} complex. The parallel and the perpendicular features indicate axially symmetric anisotropy with sixteen-lines hyperfine splitting, which is poorly resolved, due to the interaction between the electron and the vanadium nuclear spin (I=7/2). The spin Hamiltonian parameters for the complex are $g_{//} = 1.91$, $g_{\perp} = 1.93$, while the hyperfine coupling $A_{//} = 193 \times 10^{-4}$ (cm^{-1}) and $A_{\perp} = 55$, indicating that the d^1 unpaired electron is present in the d_{xy} orbital in square-pyramidal geometry [24].

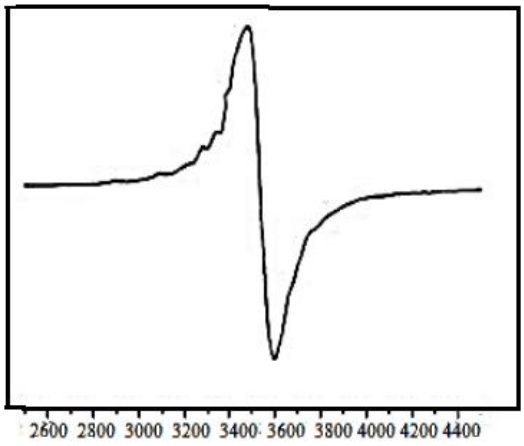

Fig. 5: ESR spectrum of [VO(Hsdhb)$_2$]

The molecular orbital coefficients α^2 and β^2 for VO^{+2} complex was calculated (eqs. 5-8);

$$A_{//} = -PK - 4\beta^2 P/7 - (g_e - g_{//})P - 3/7(g_e - g_{\perp})P \quad (5)$$

$$A_{\perp} = -PK - 4\beta^2 P/7 - 11/14(g_e - g_{\perp})P \quad (6)$$

$$g_e - g_{//} = 8\,\alpha^2\beta^2\lambda/E \quad (7)$$

$$p = 7/6(A_{//} - A_{\perp}) \quad (8)$$

P is the dipolar interaction constant between magnetic moment of the electron and vanadium nucleus [27]. The spin-orbit coupling coefficient, λ, is assumed to be 170 cm^{-1} for VO^{+2} ion and E is the electronic transition energy of $^2B_2 \rightarrow {}^2E$ and k is the Fermi contact term. It is related directly related to both the isotropic hyperfine coupling and the unpaired electron density at the nucleus. The super-exchange interaction between the two VO^{+2} ions lead to a configuration, in which the singlet state is energetically favored as the two electron spins with an anti-ferromagnetic character [24]. The values of β^2 (0.81) and α^2(0.85) indicates that the in-plane σ-bonding is less covalent, i.e., in-plane σ-bonding and inplane and π-bonding are appreciably ionic [28].

TGA

TGA diagram of H_2sdhb shows three weight loss assigned to ½ N_2 molecule (Calcd. 3.6, Found 3.5%; 140 - 244º C), C_3H_3NS, ½ O_2 and ½ H_2 species (Calcd. 26.0, Found 26.3%; 245 - 458º C) and C_7H_5N, SO_2 and ½ O_2 fragments (Calcd. 46.6; Found 46.5%; 458 – 710º C).

The TGA thermograms of the complexes (Table 2) indicate that they are decomposed in two to three steps, based on release of coordinated water, and thermal decomposition of the ligand's moieties *via* the break-down of the hetero bonds [29].

Table 2: TGA data of H_2sdhb complexes

Complex	Temperature range (°C)	Fragment loss	Calc. (%)	Found (%)
$[Co(Hsdhba)_2(H_2O)_2]$	150 - 398 399 - 972	$2H_2O$ $2C_2H_2S$, $2CHN_2$, C_6H_4, $2SO_2$	4.27 47.69	4.21 48.02
$[VO(Hsdhba)_2]$	160 - 432 433 - 983	$2C_2H_2$ $2CHN_2$, C_6H_4, $2SO_2$	6.38 35.09	6.39 35.24

Mass

The mass spectrum of H_2sdhb shows molecular ion peaks at 650.62 and 588.10 assigned to $[(H_2sdhba)(H_2sdhba\text{-}C_3H_3N_2S)]^+$ (Calcd. 651.00) and $[(H_2sdhba)(H_2sdhba\text{-}C_3H_3N_2S_2O_2)]^+$ (Calcd. 587.00), respectively.

the molecular ion peaks of the reported complexes (Table 3) confirm the 1:2 metal : ligand composition [30].

Table 3: Mass spectral data of H_2sdhb complexes

Complex	Molecular ion peak	Calc.	Found
$[Co(Hsdhba)_2(H_2O)_2]$	$[Co(Hsdhba)_2]^+$ $[Co(Hsdhba\text{-}C_2H_2N)_2]^+$ $[Co(Hsdhba\text{-}C_3H_2N_2S)_2]^+$ $[Co(Hsdhba\text{-}C_7H_6N_2S_2O_3)_2]^+$	806.90 726.90 610.90 346.90	805.01 728.00 608.99 346.81
$[Ni(Hsdhba)_2(H_2O)_2]$	$[Ni(Hsdhba\text{-}C_2H_2N)_2]^+$ $[Ni(Hsdhba\text{-}C_3H_2N_2S)_2]^+$	726.69 610.69	725.98 611.02

TOXICITY-ASSESMENT AGAINST MICROCHLOROPHYTE (Chlorella Vulgaris)

Inhibitory effects of the metal ions or their complexes on algal cells occurred *via* morphology and biochemical effects have been discussed [18,29]. The effect of H_2sdhb, $Co(AcO)_2.4H_2O$, $Ni(AcO)_2.4H_2O$, $VO(SO_4)H2O$, $[Co(Hsdhb)_2(H_2O)_2]$, $[Ni(Hsdhb)_2(H_2O)_2]$ and $[VO(Hsdhb)_2]$ on the growth of *C. vulgaris* microchlorophyte after 3 days incubation were examined (Table 4 & Fig. 6). H_2sdhba shows little effect in eco-toxicity, which may be due to inter- and intra-H bonds [18,29]. The reported complexes show higher eco-toxicity and altering the algae growth more than the free Schiff-base [18].

Table 4: EC50 values of H_2sdhb and its complexes against the growth of green alga (*Chlorella vulgaris)*

Treatment	H_2sdhb	$[Co(Hsdhb)_2(H_2O)_2]$	$[Ni(Hsdhba)_2(H_2O)_2]$	$[VO(Hsdhba)_2]$
EC_{50} (mgL^{-1})	50.01	49.92	49.90	69.81
Unit	2.0	1.83	1.81	1.32
Toxicity	Toxic	Toxic	Toxic	Toxic

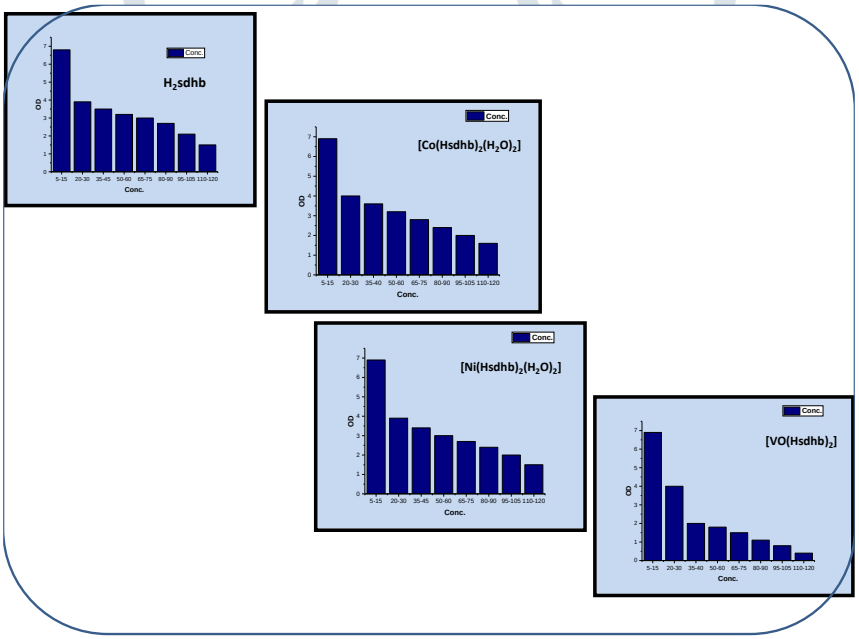

Fig. 6: Effect of H_2sdhb and its $[Co(Hsdhb)_2(H_2O)_2]$, $[Ni(Hsdhb)_2(H_2O)_2]$ and $[VO(Hsdhb)_2]$ complexes on the growth of green alga (*Chlorella vulgaris)*

Conclusion

Co(II), Ni(II) and VO^{2+} complexes containing Schiff base, sulfathiazole and 2,4-dihydroxybenzaldehyde, (H_2sdhb) were prepared and investigated using FTIR, NMR, UV-vis, ESR and mass spectroscopic, elemental

analysis, magnetic and TGA measurements. H_2sdhb acts as a didentate mononegative *via* deprotonated phenolic-O^- and azomethine-N atoms. The UV-vis. and ESR spectra indicated octahedral {Co(II) and Ni(II)} and square-pyramidal {VO^{2+}} geometries. The mass spectra and TGA thermal analysis agree with the composition of 1:2 (metal: ligand) complexes. The toxicity of free ligand and its complexes against *C. vulgaris* were also examined.

CONFLICT OF INTEREST

The authors declare no conflict of interest. This work is original research that has not been published previously and not under consideration for publication elsewhere. All the authors listed have approved the Manuscript that is enclosed. All figures in this manuscript are non-published and original. There are no personal circumstances or interest that may be perceived as inappropriately influencing the representation or interpretation of reported research results. The funders had no role in the design of the study; in the collection, analyses, or interpretation of data; in the writing of the manuscript; or in the decision to publish the results.

ACKNOWLEDGEMENTS

The authors would like to thank Dr Eglal El Metawally and Dr Nadim Saadat for running the NMR and mass spectra, respectively.

References

1. Nogrady Th., Medicinal Chemistry, 2nd ed., Oxford University Press, New York, 1988: 383.

2. Ogden R C and Flexner C W, Protease Inhibitors in AIDS Therapy, Marcel Dekker, New York, 2001.

3. Boyd A E, Sulfonylurea receptors, ion channels, and fruit flies Diabetes, 1988, 37: 847-850.

4, Owa T and Nagasu T, Novel sulphonamide derivatives for the treatment of cancer, , Expert Opin. Ther. Pat., 2000, 10: 1725-1740.

5. Ruiz M, Perello L, Ortiz R, Castineiras A, Maichlemossmer C, Canton E, Synthesis, characterization, and crystal structure of [Cu(cinoxacinate)$_2$] · $2H_2O$ complex: A square-planar CuO_4 chromophore. Antibacterial studies, J. Inorg. Biochem., 1995, 59: 801-810.

6. Salehi M, Kubicki M, Galini M, Jafari M, Malekshah R E, Synthesis, characterization and crystal structures of two novel sulfa drug Schiff base ligands derived sulfonamide and molecular docking study, Journal of Molecular Structure, 2019, 1180: 595-602.

7. Akral S and Singh V, Recent development on importance of heterocyclic amides as potential bioactive molecules: a review, Current Bioactive Compounds, 2019, 15 (3): 316–336.

8. Rama I and Selvameena R, Manganese(II), cobalt(II), nickel(II), copper(II) and zinc(II) complexes of sulfathiazole functionalised Schiff base: Synthesis, characterization, redox behavior, antioxidant and antimicrobial activities, J. Indian Chem. Soc., 2020, 97(11a):2144-2154; Saad F A, and Khedr A M, Greener solid state synthesis of nanosized mono and homo bi-nuclear Ni(II), Co(II) Mn(II), Hg(II), Cd(II) and Zn(II) complexes with new sulfa ligand as a potential antitumour and antimicrobial agents. J. Mol. Liq., 2017, 231 : 572–579.

9. Saad F A, El-Ghamry H A, Kassem M A and Khedr A M, Nano-synthesis, Biological Efficiency and DNA Binding Affinity of New Homo-binuclear Metal Complexes with Sulfa Azo Dye Based Ligand for Further Pharmaceutical Applications, Journal of Inorganic and Organometallic Polymers and Materials, 2019, 29 : 1337–1348; doi.org/10.1007/s10904-019-01098-z

10. Reiss A, Cioatera N, Dobrit,escu A, Rotaru M, Carabet A C, Parisi F, Ganescu A, Dabuleanu I, Spînu C I and Rotaru P, Bioactive Co(II), Ni(II), and Cu(II) Complexes Containing aTridentate Sulfathiazole-Based (ONN) Schiff Base, Molecules, 2021, 26: 3062; doi.org/10.3390/molecules26103062.

11. Mondal S, Mondal T K, Rajesh Y, Mandal M and Sinha C, Copper(II)-sulfonamide Schiff base complexes: Structure, biological activity and theoretical interpretation, Polyhedron, 2018, 151: 344-354.

12. Dawood F A, Yahya F L and Al-Shemary R K, Preparation and characterization of sulfathiazole Schiff-base complexes of Co(II), Ni(II), Cu(II) and Mn(II), Nat. Volatiles&Essent. Oils, 2021, 8(5): 8991-9003.

13. Ramadan A M, Bayoumi H A and Elsamra R I, Appl. Organomet. Chem., Synthesis, characterization, biological evaluation and molecular docking approach of nickel(II) complexes containing O, N- donor chelation pattern of sulfonamide-based Schiff-bases, 2021, 35(12): e6412.

14. Blaise V and Ferard J F (eds). Small-scale Freshwater Toxicity Investigations, 2005, 1: 137-179.

15. Kunisawa R R, Mandel M and Cohen-Bazire G, Purification and properties of unicellular blue-greenalgea (order chroococcales) Bacteriological reviews, 1971, 35: 171-205.

16. El Asmy H A, Butler I S and Mostafa S I, DNA interaction and anticancer evaluation of new adenine complexes in presence of N, N-donors as secondary chelate, J. Mol. Struct., 2021, 1223: 128976.

17. Geary W, The use of conductivity measurements in organic solvents for the characterisation of coordination compounds, Coord. Chem. Rev., 1971,7: 81–122 .

18. El-Emam A A, Belal A, Hussein M H and Mostafa S I, New Complexes based on Sulfathiazole; Synthesis, Characterization and Toxicity Assessment against Chlorella Vulgaris Microchlorophyte, Open Access Journal of Chemistry, 2019, 3(2): 20-33.

19. Ouf A, Ali M S, Saad E M and Mostafa S I, pH-metric and spectroscopic properties of new 4-hydroxysalicylidene-2-aminopyrimidine Schiff-base transition metal complexes, J. Mol. Struct. 2010, 973: 69–75; Ouf A, Ali M S, Sulyman M S, El-Defrawy A M and Mostafa S I, Synthesis and Characterization of New Transition Metal Complexes of Schiff-base Derived from 2-Aminopyrimidine and 2,4-Dihydroxybenzaldehyde and Its Applications in Corrosion Inhibition, J. Korean Chem. Soc., 2010, 54 : 402–410.

20. Anan N A, Hassan S M, Saad E M, Butler I S and Mostafa S I, Preparation, characterization and pH-metric measurements of 4-hydroxysalicylidene chitosan Schiff-base complexes of Fe(III), Co(II), Ni(II), Cu(II), Zn(II), Ru(III), Rh(III), Pd(II) and Au(III), Carbohydrate Research, 2011, 346: 775–793.

21. Hassan H M A, Saad E M, Soltan M S, Betiha M A, Butler I S and Mostafa S I, A palladium(II) 4-hydroxysalicylidene Schiff-base complex anchored on functionalized MCM-41: An efficient heterogeneous catalyst for the epoxidation of olefins, Applied Catalysis A: General, 2016, 488: 148-159.

22. Shabana A A, Butler I S, Gilson D F R, Jean-Claude B J, Mouhri Z S, Mostafa M M and Mostafa S I, Synthesis, characterization, anticancer activity and DNA interaction studies of new 2-aminobenzothiazole complexes; crys- tal structure and DFT calculations of $[Ag(Habt)_2]ClO_4$, Inorg. Chim. Acta, 2014, 423: 242–255.

23. Tella A C and Obaleye J A, Metal complexes as antibacterial agents: Synthesis, characterization and antibacterial activity of some 3d metal complexes of sulphadimidine, J. Chem., Campo Grande, 2010, 2 : 11-26.

24. Mostafa S I, Gabr I M, El-Asmy H A and Emam M E, Complexes of 3-aminopyrazine-2-carboxylic acid with VO^{2+} , Pd(II), W(VI) and UO_2^{2+}; preparation and characterization, Inorg. Chem. Ind. J., 2009, 4(1): 31-35.

25. Vellaiswamy G and Ramaswamy S, Synthesis, characterization and antimicrobial screening of novel Schiff-bases from sulfa drugs, Int. J. Pharm. Pharm. Scien., 2014, 6 : 487-491.

26. Mostafa S I, Perlepes S P and Hadjiliadis N, New dinuclear transition metal complexes with the [M2 (μ-dhbq)] n+ core and 2-(2′-Pyridyl) quinoxaline (L) as a terminal ligand: preparation and characterization (dhbq2-= the Dianion of 2, 5-Dihydroxy-1, 4-benzoquinone; M= AgI, MnII, CoII, NiII, CuII, RuII, PdII, FeIII, RhIII; n= 0, 2, 4), 2001, 56(4-5): 394-440

27. El-Metwally N M, El-Shazly R M, Gabr I M and El-Asmy A A, Physical and spectroscopic studies on novel vanadyl complexes of some substituted thiosemicarbazides, Spectrochimica Acta, 2005, 1113-1119; Warad D U, Statish C D, Kulkarni V H and Bajgur C S, Synthesis, Characterisation and Catalytic Studies of Iron(III), cobalt(II), nickel(II) and Cu(II) complexes containing triphenylphosphine and β-diketone, Trans. Met. Chem., 2005, 30: 433-438.

28. Demirci T B, Köseoğlu Y, Güner S and Ülküseven B, Oxovanadium(IV) complexes of bromo-and methoxy substituted *N*1,*N*4-diarylidene-*S*-methylthiosemicarbazones Central European Journal of Chemistry,2006, 4: 149-159

29. Annan N A, Butler I S, Osman Y H, Hussein M H, Jean-Claude B J, Saad E M, and Mostafa S I, Complexes based N,N-donors (2,2′-bipyridyl & 2-(2-aminophenyl)benzimidazole); Synthesis, characterization, DNA interaction and toxicity assessment against Chlorella vulgaris microchlorophyte; X-ray crystal structure of $[Zn(bpy)_3)]Cl_2$, *Inorganica Chimica Acta*, 2020, 512: 119885; doi.org/10.1016/j.ica.2020.119885.

30. Fathy A E, Butler I S, Abd El Rahman M, Jean Claude B J and. Mostafa S I, Anticancer Evaluation and Drug Delivery of New Palladium(II) Complexes Based on the Chelate of Alendronate onto Hydroxyapatite Nanoparticles, Inorg. Chim. Acta, 2018, 473: 44-50; Fathy A, Butler I. S, Abd Elrahman M, Jean Claude, B J and Mostafa S I, New Active Bisphosphonate (Etidronate) Complexes as Anticancer Agents, *Inorganic Chemistry An Indian J*ournal, 2017, 12: 119-12.